Coupled Interfacial Energy and Temperature Effects on Size-Dependent Yield Strength and Strain Hardening of Small Metallic Volumes

Rashid K. Abu Al-Rub[1]
e-mail: rabualrub@civil.tamu.edu

Abu N. M. Faruk

Zachry Department of Civil Engineering,
Texas A&M University,
College Station, TX 77843

Plasticity in heterogeneous metallic materials with small volumes is governed by the interactions of dislocations at interfaces. In particular, interfaces of a material confined in a small volume can strongly affect the mechanical properties of micro and nanosystems. In this paper, the framework of higher-order strain gradient plasticity theory with interfacial energy effect is used to investigate the coupling of interfacial energy with temperature and how it affects the initial yield strength (i.e., onset of plasticity) and the strain hardening rates of confined small metallic volumes. It is postulated that the interfacial energy decreases as temperature increases such that size effect decreases as temperature increases. As an application, the size effect of thermal loading of a film-substrate system is investigated. It is shown that the temperature at which the film starts to yield plastically is size-dependent, which is attributed to the size-dependent yield strength. Furthermore, the flow stress is more temperature sensitive as the size decreases. [DOI: 10.1115/1.4002651]

Keywords: size effect, interfaces, surface energy, temperature, thin film

1 Introduction

Plasticity in heterogeneous materials with small volumes (e.g., thin films, thin wires, grains in polycrystals, and particles in composites) is governed by the interactions of dislocations at interfaces (e.g., thin film-substrate interface, grain boundary, and particle-matrix interface). These include interactions of existing dislocations, as well as the nucleation of dislocations at an interface. The rational for interface dominated plasticity is simple: Dislocations glide through the single crystal domain with relative ease but pile-up at interfaces so that interface interactions become a critical step in continuing plastic deformation. While the details of dislocation interactions at interfaces take place at the atomic scale [1], and the behavior of dislocations in bulk is most accurately modeled by discrete dislocation dynamics (e.g., Refs. [2–4]), both of these models are much too expensive and impractical for analyzing the resulting bulk behavior. The need for a continuum (but nonclassical) framework for describing the plasticity across interfaces including the prediction of size effects seen in many experiments (e.g., Refs. [5–12]) is necessary.

The interfacial interactions can be characterized within the framework of higher-order (not lower-order) nonlocal strain gradient plasticity theory (e.g., Refs. [13–16]) through a proper interpretation of the physical nature of the higher-order interfacial boundary conditions that result from the application of the principle of virtual power (or virtual work). Recently, initial attempts have been made to relate these nonstandard boundary conditions to the *interfacial energy* at interfaces and found out that this proposition can be used successfully in predicting the increase in the initial yield strength, flow stress, and strain hardening rates with decreasing size in micro and nanostructured materials [16–19]. Abu Al-Rub [19] investigated different mathematical forms of the interfacial energy and formulated, besides the yield condition for the bulk, a yieldlike condition for the interface. However, to the authors' best knowledge, the effect of temperature on the interfacial energy and on the size effect of small-scale metallic volumes has not been investigated. Therefore, the objective of this paper is to utilize the framework of higher-order strain gradient plasticity theory, as formulated in Refs. [16,19], to investigate the coupling of interfacial energy with temperature and how it affects the initial yield strength (i.e., onset of plasticity) and the strain hardening rates of confined small metallic volumes. Particularly, the effect of cooling of a metallic thin film on a silicon substrate is investigated. It is shown that the cooling temperature at which the film starts to yield is size-dependent such that as the film thickness decreases, more cooling is needed to yield the film plastically.

This paper is organized as follows. The framework of higher-order strain gradient plasticity theory with the consideration of interfacial energy effects is outlined in Sec. 2. The temperature and functional dependence of the interfacial energy on the interfacial plastic strain is discussed in Sec. 3. In Sec. 4, the presented higher-order gradient plasticity is applied to the thermal cooling of a metallic thin film on a silicon substrate. Conclusions are outlined in Sec. 5.

2 Higher-Order Strain Gradient Plasticity With Interfacial Effects

In order to be able to model the small-scale phenomena, such as the effect of size of microstructural features on the material mechanical properties, the higher-order strain gradient plasticity theory that can predict the size scale effects is considered here. In this section, the recently developed thermodynamic framework for higher-order gradient plasticity theory by Abu Al-Rub et al. [16] is utilized to derive the necessary constitutive equations.

[1]Corresponding author.

Contributed by the Materials Division of ASME for publication in the Journal of Engineering Materials and Technology. Manuscript received March 17, 2010; final manuscript received August 12, 2010; published online December 3, 2010. Assoc. Editor: Assimina Pelegri.

In the following, Einstein index notation with summation over repeated lower indices is used unless otherwise noted. Also, the indices after a comma represent partial derivatives, and the superimposed dot indicates derivative with respect to time.

The classical theory of isotropic plastic solids undergoing small deformation allows additive decomposition of total strain rate $\dot{\varepsilon}_{ij}$ into an elastic part $\dot{\varepsilon}^e_{ij}$ and a plastic part $\dot{\varepsilon}^p_{ij}$ such that

$$\dot{\varepsilon}_{ij} = \dot{\varepsilon}^e_{ij} + \dot{\varepsilon}^p_{ij}, \quad \dot{\varepsilon}^p_{kk} = 0 \tag{1}$$

where the rate of local effective plastic strain $\dot{\varepsilon}^p$ is defined as

$$\dot{\varepsilon}^p = \sqrt{\frac{2}{3}\dot{\varepsilon}^p_{ij}\dot{\varepsilon}^p_{ij}} \tag{2}$$

The total strain rate $\dot{\varepsilon}_{ij}$ is defined by the symmetric part of the velocity gradient $v_{i,j}=\partial v_i/\partial x_j$ such that

$$\dot{\varepsilon}_{ij} = \frac{1}{2}(v_{i,j} + v_{j,i}) \tag{3}$$

The principle of virtual power asserts that given any sub-body volume Γ, the virtual power expended on Γ by materials or bodies exterior to Γ (i.e., external power) be equal to the virtual power expended within Γ (i.e., internal power) such that

$$P_{\text{ext}} = P_{\text{int}} \tag{4}$$

where P_{ext} and P_{int} are the external and internal virtual powers, respectively. Let n_i denote the outward unit normal to the surface $\partial\Gamma$. The external expenditure of power is assumed to arise from a macroscopic surface traction t_i and a scalar microtraction force q that is conjugate to the local effective plastic strain ε^p at the interface with a unit vector n_i normal to the boundary $\partial\Gamma$ of Γ. Therefore, by neglecting body forces, one can write the external virtual power in the following form:

$$P_{\text{ext}} = \int_{\partial\Gamma} (t_i v_i + q\dot{\varepsilon}^p)dA \tag{5}$$

where v_i is the velocity vector and q is defined as the derivative of the interfacial energy φ (free energy per unit area) with respect to the effective plastic strain at the interface $\varepsilon^{p(I)}$ [16–19]

$$q = \frac{\partial\varphi}{\partial\varepsilon^{p(I)}} \tag{6}$$

The interfacial energy φ introduces an interfacial resistance against dislocation motion, emission, and transmission through the interface. Moreover, $\varphi=0$ designates a free surface, where dislocations are allowed to escape, while $\varphi\to\infty$ designates a microclamped interface, where dislocations are not allowed to penetrate the interface. Hence, for intermediate interfaces, where some dislocations are blocked and some can escape, finite values for φ are obtained.

The external power is balanced by an internal expenditure of power characterized by the Cauchy stress tensor σ_{ij} defined over Γ and the drag stress R conjugate to ε^p and associated with isotropic hardening. However, to incorporate the gradients of the plastic strain, one also considers power expenditures associated with the gradient of the effective plastic strain $\nabla_k\varepsilon^p=\partial\varepsilon^p/\partial x_k$. One, therefore, can assume that additional power is expended internally by the higher-order microforce vector Q_k conjugate to $\nabla_k\varepsilon^p$. Specifically, the internal virtual power is assumed to have the following form:

$$P_{\text{int}} = \int_{\Gamma} (\sigma_{ij}\dot{\varepsilon}^e_{ij} + R\dot{\varepsilon}^p + Q_k\nabla_k\dot{\varepsilon}^p)dV \tag{7}$$

Using Eq. (1) into Eq. (7) gives

$$P_{\text{int}} = \int_{\Gamma} (\sigma_{ij}\dot{\varepsilon}_{ij} - s_{ij}\dot{\varepsilon}^p_{ij} + R\dot{\varepsilon}^p_e + Q_k\nabla_k\dot{\varepsilon}^p)dV \tag{8}$$

where $s_{ij}=\sigma_{ij}-(1/3)\sigma_{kk}\delta_{ij}$ is the deviatoric part of the Cauchy stress tensor, and due to plastic incompressibility ($\dot{\varepsilon}^p_{kk}=0$), one can write $\sigma_{ij}\dot{\varepsilon}^p_{ij}=s_{ij}\dot{\varepsilon}^p_{ij}$.

One can apply the divergence theorem along with Eq. (3) to obtain the following expressions:

$$\int_{\Gamma}\sigma_{ij}\dot{\varepsilon}_{ij}dV = \int_{\partial\Gamma}\sigma_{ij}n_j v_i dA - \int_{\Gamma}\sigma_{ij,j}v_i dV, \quad \int_{\Gamma}Q_k\nabla_k\dot{\varepsilon}^p dV = \int_{\partial\Gamma}Q_k\dot{\varepsilon}^p n_k dA - \int_{\Gamma}Q_{k,k}\dot{\varepsilon}^p dV \tag{9}$$

Substituting the above equations into Eq. (8) gives

$$P_{\text{int}} = -\int_{\Gamma}\sigma_{ij,j}v_i dV - \int_{\Gamma}[s_{ij}\dot{\varepsilon}^p_{ij} - (R - Q_{k,k})\dot{\varepsilon}^p]dV + \int_{\partial\Gamma}\sigma_{ij}n_j v_i dA + \int_{\partial\Gamma}Q_k\dot{\varepsilon}^p n_k dA \tag{10}$$

Substituting Eqs. (5) and (10) into Eq. (4) along with Eq. (2), one gets

$$\int_{\Gamma}\sigma_{ij,j}v_i dV + \int_{\partial\Gamma}(t_i - \sigma_{ij}n_j)v_i dA + \sqrt{\frac{2}{3}}\int_{\Gamma}\left[\sqrt{\frac{3}{2}s_{ij}s_{ij}} - (R - Q_{k,k})\right]\dot{\varepsilon}^p_{ij}dV + \int_{\partial\Gamma}(q - Q_k n_k)\dot{\varepsilon}^p dA = 0 \tag{11}$$

where Γ, v_i, and $\dot{\varepsilon}^p_{ij}$ can be arbitrarily specified if and only if the following four conditions are satisfied:

$$\sigma_{ij,j} = 0 \tag{12}$$

$$t_i = \sigma_{ij}n_j \tag{13}$$

$$\sqrt{\frac{3}{2}s_{ij}s_{ij}} - (R - Q_{k,k}) = 0 \tag{14}$$

$$q = Q_k n_k \tag{15}$$

Equation (12) is the macroforce equilibrium equation and Eq. (13) is the macrotraction boundary condition, whereas Eq. (14) is the nonlocal yield criterion and Eq. (15) is the microtraction boundary condition at interfaces.

Based on the laws of thermodynamics, Abu Al-Rub et al. [16] expressed the drag stress R and the higher-order microforce Q_k in the following forms in order to obtain Aifantis [20] gradient plasticity theory:

$$R = \sigma_y + h\varepsilon^p \quad \text{and} \quad Q_k = h\ell^2\nabla_k\varepsilon^p \tag{16}$$

where σ_y is the size-independent yield stress, h is the hardening modulus, and ℓ is the material length scale parameter that can physically be related to the average dislocation free-path [21,22]. Other more general forms for R and Q_k can be derived, as shown in Ref. [16]. However, the Aifantis [20] model is considered here for simplicity.

Taking the divergence of Q_k in Eq. (16) yields

$$Q_{k,k} = h\ell^2\nabla^2\varepsilon^p \tag{17}$$

where $\nabla^2=\partial^2/\partial x_k\partial x_k$ is the Laplacian operator. Therefore, Eq. (14) becomes

$$\sqrt{\frac{3}{2}s_{ij}s_{ij}} - (\sigma_y + h\varepsilon^p) + h\ell^2\nabla^2\varepsilon^p = 0 \Rightarrow \sigma = \sigma^H - h\ell^2\nabla^2\varepsilon^p \tag{18}$$

where $\sigma = \sqrt{(3/2)s_{ij}s_{ij}}$ and σ^H are the effective von Mises and the homogeneous part of the effective stress.

Also, from Eqs. (15) and (16) along with Eq. (6), one can write

$$q = \frac{\partial \varphi}{\partial \varepsilon^{p(I)}} = h\ell^2\nabla_k\varepsilon^p n_k \tag{19}$$

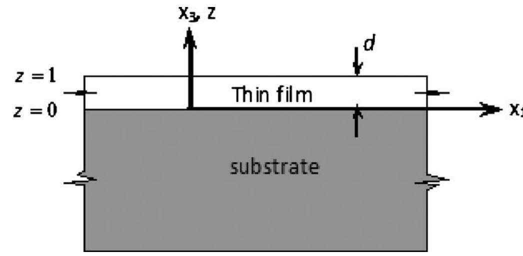

Fig. 1 An elastoplastic thin film of thickness *d* on an elastic substrate

3 Temperature and Functional Dependence of the Interfacial Energy

Different expressions for the interfacial energy φ can be assumed based on the interface characteristics, as presented by Abu Al-Rub [19]. However, in this paper, the following temperature-dependent expression for the interfacial energy is assumed:

$$\varphi = \left[\gamma\varepsilon^{p(I)} + \frac{1}{2}\beta(\varepsilon^{p(I)})^2\right] f(T) \tag{20}$$

where γ is the temperature-independent interfacial yield strength, which characterizes the stiffness of the interface boundary in blocking dislocations from crossing the interface (i.e., the surface tension of the interface), β is another temperature-independent interfacial property, which characterizes the interfacial hardening that results during the transmission of dislocation pile-ups across the interface, and $f(T)$ is a temperature-dependent function that gives the functional dependence of φ on temperature T. A proper expression for $f(T)$ is postulated in the following. Therefore, if $\gamma=0$, the interface would yield at the same time as the bulk and consequently the interfacial effect is controlled by the interfacial hardening parameter β. Whereas, if $\beta=0$, the interface would yield at a different time than the bulk but the interface does not harden. However, it is argued in Ref. [19] that both γ and β should be scaled by another length scale; the interfacial length scale $\ell^{(I)}$ such that $\gamma=\ell^{(I)}\sigma_y$ and $\beta=\ell^{(I)}h$. Therefore, both the surface tension and the hardening of the interface are altered simultaneously by the length scale $\ell^{(I)}$. The physical origin of $\ell^{(I)}$ was discussed by Abu Al-Rub [19].

The temperature-dependency of the interfacial energy, as provided by the function $f(T)$ in Eq. (20), can be assumed as

$$f(T) = (1 - T/T_y)^\alpha \tag{21}$$

with T_y being the bulk scale-independent temperature at the onset of yield and $0 \le \alpha < 1$ is the thermal exponent. Equation (21) implies that the interfacial energy decreases as the temperature increases. Therefore, when $T=T_y$, the interface behaves like a free surface with zero interfacial energy, implying that dislocations are nucleated within the bulk and did not yet reach the interface. The functional dependence of the interfacial energy in Eq. (21) is analogous to that proposed by Cahn and Hilliard [23] for heterogeneous domains in which T_y is interpreted as the critical temperature at which the thickness of the interface becomes infinite. In fact, in Eq. (21), T_y is included just as a normalizing parameter in order not to introduce an additional material parameter that needs to be calibrated against careful experimental data. In Eq. (21), only the α parameter needs to be identified in order to include the temperature-dependency of the interfacial energy. Therefore, one might select another temperature other than T_y to normalize the temperature-dependency term in Eq. (21). However, including T_y, which will be shown later to depend on the material properties of joined materials at interfaces, implies that the interfacial properties might be a function of the thermomechanical properties of the adjacent materials along with additional parameters that characterize the distinct thermomechanical behavior of the interface. These arguments need to be verified through novel experimental setups for extracting the thermomechanical properties of interfaces.

Substituting Eq. (20) into Eq. (19) gives

$$h\ell^2\nabla_k\varepsilon^{p(I)}n_k = (\gamma + \beta\varepsilon^{p(I)})(1 - T/T_y)^\alpha \tag{22}$$

which defines the higher-order boundary condition at the interface. It is noteworthy that Eq. (22) also defines an interfacial yield condition similar to the yield condition of the bulk. Therefore, this nonclassical yield condition can be used to determine the stress at which the interface begins to deform plastically and hardens. This means that if $h\ell^2\nabla_k\varepsilon^{p(I)}n_k < \gamma(1-T/T_y)^\alpha$, then the interface is impenetrable to dislocations and no plastic deformation is developed at the interface. Once $h\ell^2\nabla_k\varepsilon^{p(I)}n_k = \gamma(1-T/T_y)^\alpha$, the interface yields plastically such that the plastic strain at the interface is not zero and the interfacial hardening should be activated. Then the interface continues to deform plastically as long as $h\ell^2\nabla_k\varepsilon^{p(I)}n_k > \gamma(1-T/T_y)^\alpha$ in a nonlinear hardening mode characterized by $\beta(1-T/T_y)^\alpha$.

4 Application to Thermal Loading of a Metallic Thin Film on a Substrate

The problem of a thin film of thickness d on a semi-infinite substrate subjected to thermal loading will be studied now (see Fig. 1). A quasi-static monotonic thermal loading is imposed by cooling the film-substrate system from an initial temperature T_o at which the film and substrate are stress-free and dislocation-free. The substrate undergoes unconstrained contraction but due to the mismatch between the thermal-expansion coefficient of the film α_f and the substrate α_s, stress develops in the film, which is tensile for $\alpha_f > \alpha_s$.

Since the film is infinitely long in the x_1-direction and initially homogeneous, the solution depends only on x_3 such that by assuming a plane strain problem in the x_2-direction, one can write

$$\sigma_{33} = \sigma_{13} = 0 \quad \text{and} \quad \sigma_{11} = \sigma_o(x_3) \tag{23}$$

where the stress field $\sigma_o(x_3)$ is nonuniform and unknown at this stage. Because of symmetry and because the strain components do not depend on x_1, the total strain $\varepsilon_{11}=\varepsilon_o$ must be uniform throughout the film's length such that the effective plastic strain ε^p and its Laplacian $\nabla^2\varepsilon^p$ in this case can be assumed as follows:

$$\varepsilon^p = \varepsilon_o^p(x_3) \quad \text{and} \quad \nabla^2\varepsilon^p = \varepsilon_{o,33}^p \tag{24}$$

where $\varepsilon_{o,33}^p = \partial^2\varepsilon_o^p/\partial x_3^2$. For a plane strain condition, the stress-strain relationship can be expressed as follows:

$$\sigma_o(x_3) = \frac{E}{1-\nu^2}\varepsilon_o^e(x_3) \tag{25}$$

where E is the Young modulus and ν is the Poisson ratio. The total strain in the film can be decomposed into elastic, plastic, and thermal components given by

$$\varepsilon_o = \varepsilon_o^e + \varepsilon_o^p + (1+\nu)\alpha_f\Delta T \tag{26}$$

where $\Delta T=T-T_o$ is the temperature change and the term $(1+\nu)$ is a result of the plan strain assumption. Compatibility of deforma-

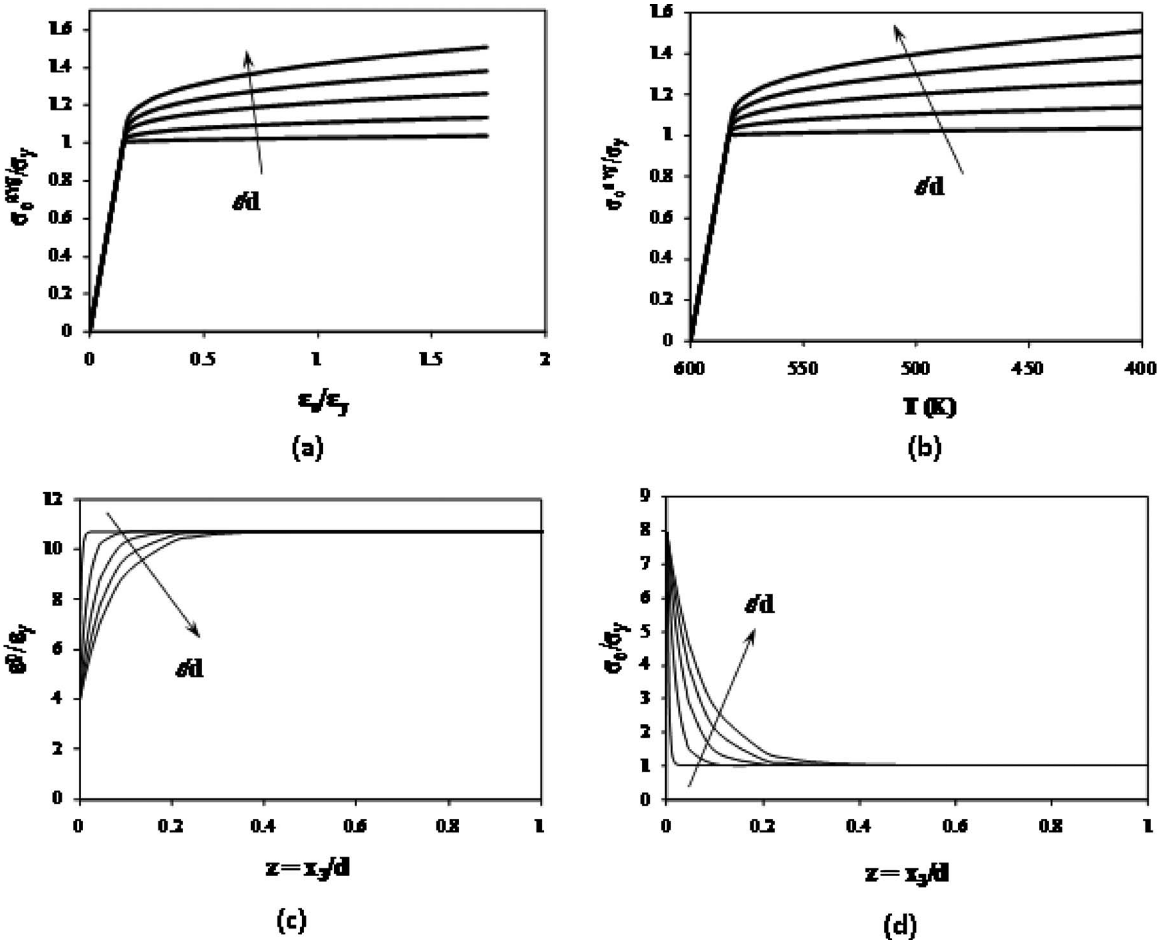

Fig. 2 Thermal cooling of an aluminum-silicon thin film-substrate system by 200 K due to interfacial yield strength only ($\delta_1=0.35$ and $\delta_2=0$). Different film thicknesses are represented by ℓ/d=0.1, 0.5, 1, 1.5, and 2 for: (*a*) average stress versus strain, (*b*) average stress and temperature, (*c*) plastic strain through the thickness, and (*d*) stress through the thickness.

tion between the film and the substrate requires that ε_o be the same and uniform throughout the film's length. The total strain in the substrate is given by

$$\varepsilon_o = (1+\nu)\alpha_s \Delta T \tag{27}$$

In Eqs. (26) and (27), $\nu_f=\nu_s=\nu$ is assumed. Substituting ε_o^e from Eqs. (26) and (27) into Eq. (25) yields

$$\sigma_o(x_3) = \frac{E}{1-\nu^2}[(1+\nu)(\alpha_s-\alpha_f)\Delta T - \varepsilon_o^p(x_3)] \tag{28}$$

In the elastic range, the above equation can be utilized to relate the yield stress with the temperature at the onset of yield (i.e., by substituting $T=T_y$ when $\sigma_o=\sigma_y$) by setting $\varepsilon_o^p=0$ in Eq. (28) such that

$$\sigma_y = \frac{E}{1-\nu}(\alpha_s-\alpha_f)(T_y-T_o) \tag{29}$$

Following from the yield condition in Eq. (18) with Eqs. (23) and (24), one gets

$$\sigma_o - \sigma_y - h\varepsilon_o^p + h\ell^2 \varepsilon_{o,33}^p = 0 \tag{30}$$

Substituting Eq. (28) into Eq. (30) along with Eq. (29) yields the following ordinary differential equation for $\varepsilon_o^p(x_3)$:

$$\varepsilon_{o,33}^p - \frac{1}{\ell^2}\left[1+\frac{E/h}{(1-\nu^2)}\right]\varepsilon_o^p = \frac{E/h}{\ell^2(1-\nu)}(\alpha_f-\alpha_s)(T-T_y) \tag{31}$$

The above equation is more conveniently expressed as a nondimensional form with the aid of variable substitution (i.e., $z=x_3/d$) such that

$$\varepsilon_{o,zz}^p - \lambda^2 \varepsilon_o^p = -F \tag{32}$$

with the constant, coefficients λ and F are given through

$$\lambda^2 = \frac{1}{(\ell/d)^2}\left[1+\frac{E/h}{(1-\nu^2)}\right] \quad \text{and} \quad F = \frac{E/h}{(\ell/d)^2(1-\nu)}(\alpha_f-\alpha_s)(T_y - T) \tag{33}$$

Equations (19)–(22) specify the higher-order boundary conditions for the current problem. At the film-free surface ($x_3=d$), $q=h\ell^2\varepsilon_{0,3}^p=0$ and at the film-substrate interface ($x_3=0$), $q=h\ell^2\varepsilon_{0,3}^p=[\gamma+\beta\varepsilon_0^{p(I)}]f(T)$. Therefore, the dimensionless boundary conditions for the problem are

$$\varepsilon_{o,z}^p|_{z=1} = 0 \tag{34}$$

$$(\ell/d)\varepsilon_{o,z}^p|_{z=0} = [\delta_1\sigma_y/h + \delta_2\varepsilon_o^p|_{z=0}]f(T) \tag{35}$$

where $\delta_1=\gamma/\sigma_y\ell$ and $\delta_2=\beta/h\ell$ are the nondimensional interfacial strength and hardening, respectively. Solution to the differential equation with the stated boundary conditions can be obtained as

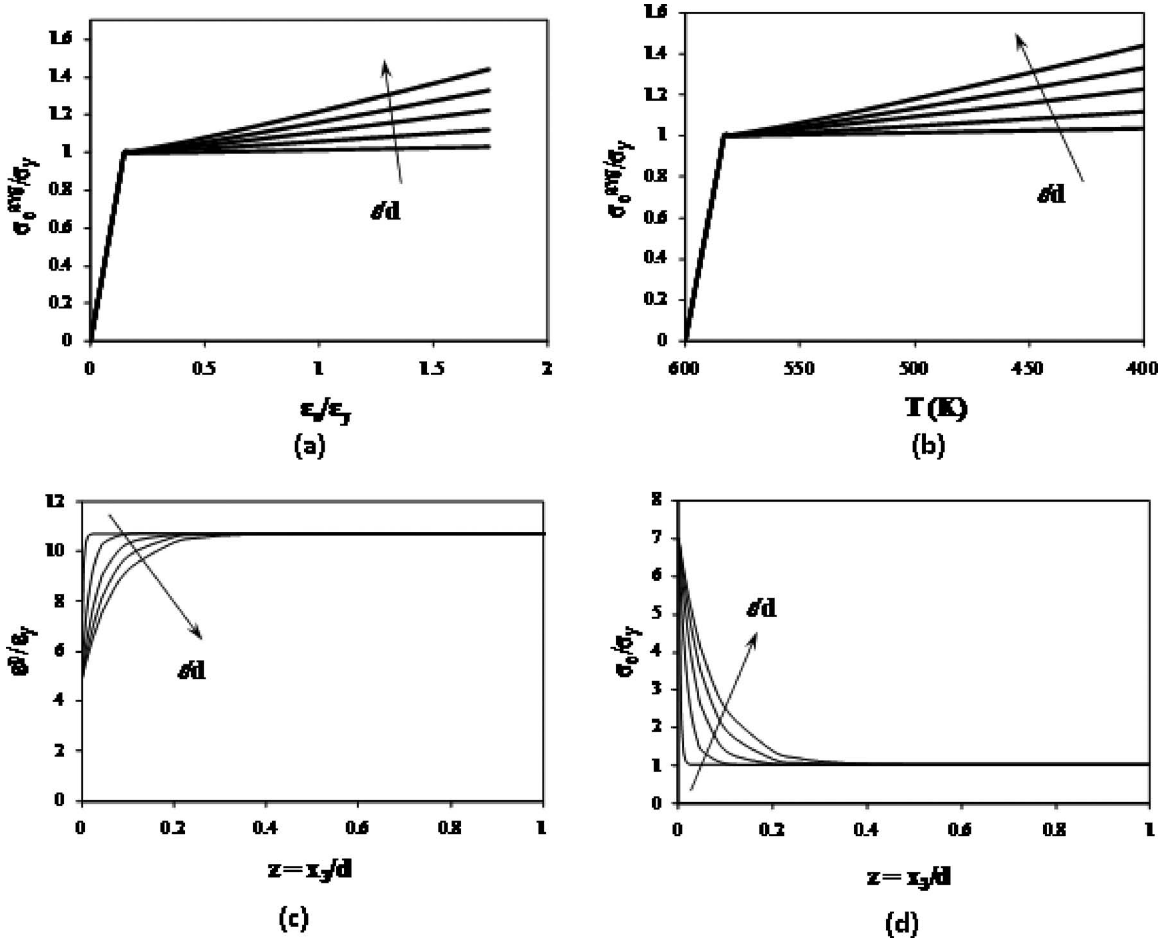

Fig. 3 Thermal cooling of an aluminum-silicon thin film-substrate system by 200 K due to interfacial hardening only ($\delta_1=0$ and $\delta_2=50$). Different film thicknesses are represented by $\ell/d=0.1$, 0.5, 1, 1.5, and 2 for: (*a*) average stress versus strain, (*b*) average stress and temperature, (*c*) plastic strain through the thickness, and (*d*) stress through the thickness.

$$\varepsilon_o^p(z) = \frac{F}{\lambda^2} + \frac{[\delta_1(\sigma_y/h) + \delta_2(F/\lambda^2)]f(T)}{\lambda(\ell/d) + \delta_2 f(T)\coth\lambda}[\sinh\lambda z - \coth\lambda\cosh\lambda z] \quad (36)$$

which can be rewritten after substituting Eq. (33) as follows:

$$\varepsilon_o^p(z) = \frac{\delta_1 f(T)\sigma_y/h}{\lambda(\ell/d) + \delta_2 f(T)\coth\lambda}[\sinh\lambda z - \coth\lambda\cosh\lambda z] + \frac{(1+\nu)(E/h)(\alpha_f-\alpha_s)(T_y-T)}{(1-\nu^2)+E/h}\left[1 + \frac{\delta_2 f(T)(\sinh\lambda z - \coth\lambda\cosh\lambda z)}{\lambda(\ell/d)+\delta_2 f(T)\coth\lambda}\right] \quad (37)$$

Substituting the above equation into Eq. (28) yields a linear relationship between σ_o and T as follows:

$$\sigma_o(z) = \sigma_n - c(\sinh\lambda z - \coth\lambda\cosh\lambda z) \quad (38)$$

with

$$\sigma_n = \frac{E}{1-\nu}(\alpha_f-\alpha_s)\left[(T_o-T) - \frac{(T_y-T)}{1+(1-\nu^2)(h/E)}\right] \quad (39)$$

$$c = \frac{E}{1-\nu^2}f(T)\left[\frac{\delta_1\sigma_y/h + \delta_2 F/\lambda^2}{\lambda(\ell/d)+\delta_2 f(T)\coth\lambda}\right] \quad \text{with} \quad \frac{F}{\lambda^2} = \frac{(1+\nu)E/h}{(1-\nu^2)+E/h}(\alpha_f-\alpha_s)(T_y-T) \quad (40)$$

Integrating Eqs. (37) and (38) over the thickness of the film (i.e., from $z=0$ to $z=1$) gives the average plastic strain $\varepsilon_o^{p,\text{avg}}$ and average stress σ_o^{avg} such that

$$\varepsilon_o^{p,\text{avg}} = \frac{F}{\lambda^2} - \left(\frac{1-\nu^2}{E}\right)\frac{c}{\lambda} \quad (41)$$

$$\sigma_o^{\text{avg}} = \sigma_n + \frac{c}{\lambda} \quad (42)$$

The results are analyzed for the case of cooling of an aluminum film on a silicon substrate from an initial temperature of $T_o=600$ K to $T=400$ K. Typical properties of aluminum are adopted ($E=70$ GPa, $\nu=0.33$, $\alpha_f=23.3\times10^{-6}$/K, $\sigma_y=36$ MPa, and $h=100$ MPa). Thermal expansion coefficient for silicon is taken to be $\alpha_s=3.0\times10^{-6}$/K. The thermal exponent in Eq. (21) is assumed $\alpha=0.3$. The temperature at which yielding occurs is calculated from Eq. (29) to be $T_y=582.94$ K. Film thicknesses are varied as $\ell/d=0.1$, 0.5, 1.0, 1.5, and 2. To study the influence of

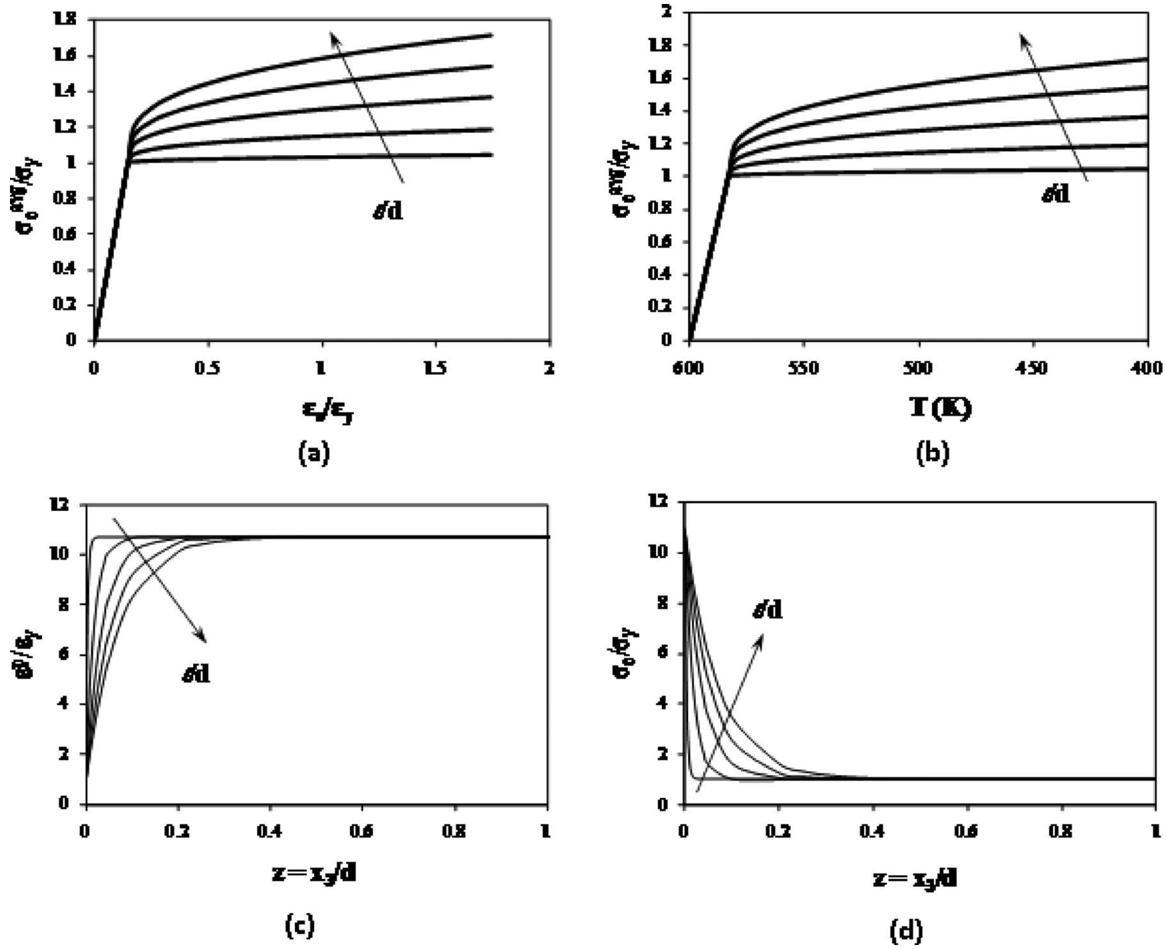

Fig. 4 Thermal cooling of an aluminum-silicon thin film-substrate system by 200 K due to both interfacial yield strength and hardening ($\delta_1=\delta_2=0.5$). Different film thicknesses are represented by $\ell/d=0.1$, 0.5, 1, 1.5, and 2 for: (*a*) average stress versus strain, (*b*) average stress and temperature, (*c*) plastic strain through the thickness, and (*d*) stress through the thickness.

the interfacial yield strength γ and interfacial hardening β, various combinations of $\delta_1=\gamma/\sigma_y\ell$ and $\delta_2=\beta/h\ell$ are assumed in the preceding analytical expressions.

Figure 2 shows the influence of interfacial yield strength alone by setting the interfacial hardening $\delta_2=0$. The normalized interfacial yield strength is assumed $\delta_1=0.35$, which corresponds to a compliant interface at which some dislocations are allowed to transmit through the interface. Figure 2(*a*) shows the normalized stress-strain relationship (average stress from Eq. (42) versus total strain from Eq. (27)). This figure shows that the initial yield stress (i.e., onset of plasticity) as well as the strain hardening rate (i.e., the tangent modulus at specific strain after yielding) are size-dependent. This is different than the conclusions in Ref. [19], where the strain hardening rate does not change with size in case the interfacial hardening is neglected (i.e., $\delta_2=0$). This obtained size-dependent strain hardening rate is induced by the temperature term $f(T)$ introduced in the interfacial energy expression in Eq. (20). Furthermore, Fig. 2(*b*) shows the variation of the normalized average stress with the variation in cooling temperature. It can be seen that during the initial cooling, the film deforms elastically until a certain level of tensile stress is reached when it starts deforming plastically. Therefore, it is interesting to note that the cooling temperature at which the film first yields (i.e., at onset of plasticity) is also size-dependent such that as the film thickness decreases, more cooling is needed to yield the film plastically. Furthermore, it can be seen from Fig. 2(*b*) that the flow (or yield) stress is more temperature sensitive as the film's thickness decreases. For examples, for the largest size considered (i.e., $\ell/d=0.1$), the flow stress remains relatively athermal (i.e., temperature-independent) as compared with the smallest size considered (i.e., $\ell/d=1.5$). Figures 2(*c*) and 2(*d*) show the final normalized variation of the plastic strain and stress across the film thickness, respectively. One can notice that the stress increases and the plastic strain decreases as the film-substrate interface is approached. These results are in good agreement with the discrete dislocation simulations by Nicola et al. [3]. Also, one can see from these figures the development of a boundary layer in which plastic strain gradients are localized. The thickness of the boundary layer increases as the size decreases. Also, one case notice that the plastic strain at the interface (i.e., at $z=0$) is not zero such that the interface behaves as a compliant interface, allowing dislocation transmission across the interface. Due to the lower plasticity at the interface as compared with the free surface of the film, the maximum stress is seen at the interface.

Next, the effect of interfacial hardening is studied by setting $\delta_1=0$ (interface yields at the same time as the bulk of the film), while the normalized interfacial hardening is assumed $\delta_2=50$ that again corresponds to a compliant interface. The corresponding results to those in Fig. 2 are shown in Fig. 3. In this case also, size effect is observed on the flow stress and strain hardening rate. The increment in tangential modulus is attributed to the presence of interfacial hardening through the nonzero δ_2 value. However, one can notice from, respectively, Figs. 3(*a*) and 3(*b*) that the yield strength and the yielding temperature are size-independent, which is different than that seen in Figs. 2(a) and 2(b). Although the overall stress-strain responses in Figs. 2(a) and 3(a) and the stress-temperature responses in Figs. 2(b) and 3(b) are very different, the plastic strain distributions in Figs. 2(c) and 3(c) and the stress distributions in Figs. 2(d) and 3(d) are qualitatively similar. A boundary layer is formed, whose thickness increases as the film's thickness decreases.

Finally, the combined effect of the interfacial yield strength and interfacial hardening is examined. Figure 4 shows the responses for $\delta_1=\delta_2=\ell^{(I)}/\ell=0.5$. As argued by Abu Al-Rub [19], for finite δ_1 and δ_2, one cannot vary one independent of the other since increasing δ_2 and fixing δ_1 will decrease the initial yield stress with decreasing size, which is not in agreement with experimental results. Therefore, both δ_1 and δ_2 should be scaled with $\ell^{(I)}$. One can see from Fig. 4(a) that both the yield strength and the strain hardening rates increase as the film's thickness decreases. This is qualitatively similar to that seen in Fig. 2(a); however, a more pronounced increase in strain hardening rate is seen in Fig. 4(a). Also, this is in qualitative agreement with experimental observations in Refs. [5,9,10,12]. Furthermore, similar to Fig. 2(b), Fig. 4(b) shows that the cooling temperature necessary to initiate yielding is size-dependent, which is attributed to the size-dependent yield strength seen in Fig. 4(a). Similar to Figs. 2(b), 2(c), 3(b), and 3(c), Figs. 4(b) and 4(c) show the formation of a boundary layer thickness, where plastic strain gradients are significant.

It is noteworthy that the above conclusions and observations are valid even if a zero value for the thermal exponent α in Eq. (21) is assumed. However, as α increases, the size effect on the yield strength and strain hardening rates decreases. Therefore, it will be interesting to validate the postulated expression for the temperature-dependent interfacial energy in Eq. (20) from experimental data. Moreover, the aforementioned conclusions are also valid under thermal heating.

5 Conclusions

Free surfaces and interfaces of a material confined in a small volume or structure can strongly affect the mechanical properties of micro and nanosystems. In this paper, the temperature and functional dependence of the interfacial energy of an interface is investigated within the framework of higher-order strain gradient plasticity theory. The higher-order (nonclassical) boundary conditions that results from the mathematical consistency of strain gradient plasticity theory are interpreted as microtraction forces that are related to the interfacial energy at the interface. The interfacial energy is a measure of the interface resistance to dislocation motion, transmission, and emission. A distinctive feature of this proposition is that interfaces can follow their own yield behavior, and depending on the form of the interfacial energy, an interfacial yieldlike condition is proposed as well as a corresponding interfacial yield stress, which indicates the stress at which dislocations begin crossing the interface, can be calculated.

It is postulated that the interfacial energy decreases as the temperature increases. This implies that size effect on the yield strength (i.e., on onset of plasticity) and strain hardening rate decreases as temperature increases. The proposed framework is applied to thermal cooling of a film-substrate system. It is concluded that the postulated interfacial energy expression provides qualitative agreements with experimental observations such that the yield strength, strain hardening rates, and yielding temperature (i.e., the temperature at which the film yields plastically) are size-dependent. Furthermore, it is concluded that the flow stress is more temperature sensitive as the film's thickness decreases.

Acknowledgment

The work reported in this paper is supported by a joint grant from the U.S. National Science Foundation and the U.S. Department of Energy (NSF Grant No. 0728032). Also, this paper is supported by a grant from the U.S. Army Research Office. These supports are gratefully acknowledged.

References

[1] Spearot, D. E., Jacob, K. I., and McDowell, D. L., 2005, "Nucleation of Dislocations From [001] Bicrystal Interfaces in Aluminum," Acta Mater., **53**, pp. 3579–3589.
[2] Khraishi, T. A., and Zbib, H. M., 2002, "Dislocation Dynamics Simulations of the Interaction Between a Short Rigid Fiber and a Glide Circular Dislocation Pile-Up," Comput. Mater. Sci., **24**, pp. 310–322.
[3] Nicola, L., Van der Giessen, E., and Needleman, A., 2003, "Discrete Dislocation Analysis of Size Effects in Thin Films," J. Appl. Phys., **93**, pp. 5920–5928.
[4] Akasheh, F., Zbib, H. M., Hirth, J. P., Hoagland, R. G., and Misra, A., 2007, "Dislocation Dynamics Analysis of Dislocation Intersections in Nanoscale Metallic Multilayered Composites," J. Appl. Phys., **101**, p. 084314.
[5] Venkatraman, R., and Bravman, J. C., 1992, "Separation of Film Thickness and Grain-Boundary Strengthening Effects in Al Thin-Films on Si," J. Mater. Res., **7**, pp. 2040–2048.
[6] Lloyd, D. J., 1994, "Particle Reinforced Aluminum and Magnesium Matrix Composites," Int. Mater. Rev., **39**, pp. 1–23.
[7] Ma, Q., and Clarke, D. R., 1995, "Size Dependent Hardness in Silver Single Crystals," J. Mater. Res., **10**, pp. 853–863.
[8] Stölken, J. S., and Evans, A. G., 1998, "A Microbend Test Method for Measuring the Plasticity Length Scale," Acta Mater., **46**, pp. 5109–5115.
[9] Haque, M. A., and Saif, M. T. A., 2003, "Strain Gradient Effect in Nanoscale Thin Films," Acta Mater., **51**, pp. 3053–3061.
[10] Espinosa, H. D., Prorok, B. C., and Peng, B., 2004, "Plasticity Size Effects in Free-Standing Submicron Polycrystalline FCC Films Subjected to Pure Tension," J. Mech. Phys. Solids, **52**, pp. 667–689.
[11] Uchic, M. D., Dimiduk, D. M., Florando, J. N., and Nix, W. D., 2004, "Sample Dimensions Influence Strength and Crystal Plasticity," Science, **305**, pp. 986–989.
[12] Xiang, Y., and Vlassak, J. J., 2006, "Bauschinger and Size Effects in Thin-Film Plasticity," Acta Mater., **54**, pp. 5449–5460.
[13] Shizawa, K., and Zbib, H. M., 1999, "A Thermodynamical Theory of Gradient Elastoplasticity With Dislocation Density Tensor. I: Fundamentals," Int. J. Plast., **15**, pp. 899–938.
[14] Gurtin, M. E., 2003, "On a Framework for Small-Deformation Viscoplasticity: Free Energy, Microforces, Strain Gradients," Int. J. Plast., **19**, pp. 47–90.
[15] Gurtin, M. E., and Needleman, A., 2005, "Boundary Conditions for Small Deformation, Single Crystal Plasticity That Account for the Burgers Vector," J. Mech. Phys. Solids, **53**, pp. 1–31.
[16] Abu Al-Rub, R. K., Voyiadjis, G. Z., and Bammann, D. J., 2007, "A Thermodynamic Based Higher-Order Gradient Theory for Size Dependent Plasticity," Int. J. Solids Struct., **44**, pp. 2888–2923.
[17] Fredriksson, P., and Gudmundson, P., 2005, "Size-Dependent Yield Strength of Thin Films," Int. J. Plast., **21**, pp. 1834–1854.
[18] Aifantis, K. E., and Willis, J. R., 2005, "The Role of Interfaces in Enhancing the Yield Strength of Composites and Polycrystals," J. Mech. Phys. Solids, **53**, pp. 1047–1070.
[19] Abu Al-Rub, R. K., 2008, "Interfacial Gradient Plasticity Governs Scale-Dependent Yield Strength and Strain Hardening Rates in Micro/Nano Structured Metals," Int. J. Plast., **24**, pp. 1277–1306.
[20] Aifantis, E. C., 1984, "On the Microstructural Origin of Certain Inelastic Models," ASME J. Eng. Mater. Technol., **106**, pp. 326–330.
[21] Abu Al-Rub, R. K., and Voyiadjis, G. Z., 2004, "Analytical and Experimental Determination of the Material Intrinsic Length Scale of Strain Gradient Plasticity Theory From Micro- and Nano-Indentation Experiments," Int. J. Plast., **20**, pp. 1139–1182.
[22] Abu Al-Rub, R. K., 2007, "Prediction of Micro and Nanoindentation Size Effect From Conical or Pyramidal Indentation," Mech. Mater., **39**, pp. 787–802.
[23] Cahn, J. W., and Hilliard, J. E., 1958, "Free Energy of a Nonuniform System. I. Interfacial Free Energy," J. Chem. Phys., **28**, pp. 258–267.